

Dynamic equilibration of airway smooth muscle contraction during physiological loading

JEANNE LATOURELLE, BEN FABRY, AND JEFFREY J. FREDBERG

Physiology Program, Harvard School of Public Health, Boston, Massachusetts 02115

Received 13 November 2000; accepted in final form 17 September 2001

Latourelle, Jeanne, Ben Fabry, and Jeffrey J. Fredberg. Dynamic equilibration of airway smooth muscle contraction during physiological loading. *J Appl Physiol* 92: 771–779, 2002; 10.1152/jappphysiol.01090.2000.—Airway smooth muscle contraction is the central event in acute airway narrowing in asthma. Most studies of isolated muscle have focused on statically equilibrated contractile states that arise from isometric or isotonic contractions. It has recently been established, however, that muscle length is determined by a dynamically equilibrated state of the muscle in which small tidal stretches associated with the ongoing action of breathing act to perturb the binding of myosin to actin. To further investigate this phenomenon, we describe in this report an experimental method for subjecting isolated muscle to a dynamic microenvironment designed to closely approximate that experienced in vivo. Unlike previous methods that used either time-varying length control, force control, or time-invariant auxotonic loads, this method uses transpulmonary pressure as the controlled variable, with both muscle force and muscle length free to adjust as they would in vivo. The method was implemented by using a servo-controlled lever arm to load activated airway smooth muscle strips with transpulmonary pressure fluctuations of increasing amplitude, simulating the action of breathing. The results are not consistent with classical ideas of airway narrowing, which rest on the assumption of a statically equilibrated contractile state; they are consistent, however, with the theory of perturbed equilibria of myosin binding. This experimental method will allow for quantitative experimental evaluation of factors that were previously outside of experimental control, including sensitivity of muscle length to changes of tidal volume, changes of lung volume, shape of the load characteristic, loss of parenchymal support and inflammatory thickening of airway wall compartments.

transpulmonary pressure; static equilibrium length; bronchoconstriction; asthma

OSCILLATORY STRESSES AND STRAINS are imposed continuously on airway smooth muscle (ASM) by the tidal action of breathing and on muscular arteries and arterioles by the pulsatile action of the heart. Smooth muscles in the urethra, urinary bladder, and gut are also subjected to periodic stretches. Dynamic loading is an intrinsic part of smooth muscle physiology.

In the case of ASM, the effects of oscillatory loads were first addressed by Sasaki and Hoppin (27) and later by Gunst and colleagues (5, 6, 8, 34), who demonstrated that imposition of tidal changes in muscle length depresses active force. Subsequent studies showed that imposed fluctuations of muscle length about a fixed mean length cause a graded depression of muscle force F and muscle stiffness E (averaged over the stretch), and augmentation of the specific rate of ATP utilization and the hysteresivity η (equivalent to the loss tangent, related to the viscosity, and a rough index of bridge cycling rate) (3, 4). Also, imposed force fluctuations about a fixed mean distending force systematically biases the ASM toward lengthening; this phenomenon has been called fluctuation-driven muscle lengthening (3).

In this report, we focus on the muscle load, its nonlinear force-length characteristic, and especially its changes in time. To do this, we considered isolated muscle loaded by a servo-controller that could closely approximate the dynamic loading conditions that are thought to prevail in vivo. This was done by using the known relationship between bronchial radius (and thus muscle length) and peribronchial stress (determined by the shear modulus of the lung parenchyma and the departure of muscle length from lung volume). We used theories developed by Macklem (19) and Lambert et al. (15), which include the pressure-area relationship of the airway and Lai-Fook's measurements of the parenchymal shear modulus and its dependence on transpulmonary pressure (PL) (11, 12).

Taken together, this information is sufficient to construct a virtual load representing that presented to the ASM by the airway wall and surrounding lung parenchyma in vivo. We used this virtual microenvironment not simply as a theory, as did Lambert and colleagues (15) and Macklem (19), but rather as an experimental working load. To do this, we expressed this virtual load mathematically and then integrated it into a servo-controlled lever system attached to maximally activated ASM isolated in a muscle bath. We then made this system "breathe" by varying PL in time. In this apparatus, the muscle was free to accommodate its instantaneous length and force according to the time-

Address for reprint requests and other correspondence: J. J. Fredberg, Physiology Program, Harvard School of Public Health, 665 Huntington Ave., Boston, MA 02115 (E-mail: jfredber@hsph.harvard.edu).

The costs of publication of this article were defrayed in part by the payment of page charges. The article must therefore be hereby marked "advertisement" in accordance with 18 U.S.C. Section 1734 solely to indicate this fact.

varying virtual load that was mechanically in series with it.

The strength of this method is that factors such as the pattern of breathing, thickening of airway wall compartments, and changes of parenchymal elastic support are represented mathematically within the servo-controller and are therefore under experimental control. As such, the sensitivity of smooth muscle shortening to changes of these factors can be measured. We considered narrowing of circular, noncartilaginous, intraparenchymal airways, and used isolated tracheal smooth muscle as a proxy to represent the contractile components within the wall of such airways. In this report, we limit attention to the method itself, the nonlinearity of the elastic load, and its changes in time.

METHODS

Setting muscle load. ASM *in vivo* shortens against a load that changes as the muscle shortens; the load is auxotonic. Earlier studies have considered muscle shortening by using linear, exponential, sigmoidal, or logarithmic elastic loads, all of which were time invariant (10, 18). These studies have shown that the degree of muscle shortening that is achieved during auxotonic loading is a function of not only the final load (force) imposed on the muscle but also of the shape of the force-length load characteristic (10, 18). Here we describe a more physiological load characteristic and, importantly, its changes in time.

ASM *in situ* is tethered elastically to the lung parenchymal tissues that surround the airway. The lung parenchyma is deformable, and this deformability comes into play in two ways. First, for a given fixed PL, parenchymal deformability determines how the peribronchial stress varies as ASM shortens. Second, for a given fixed smooth muscle length, parenchymal deformability determines how the peribronchial stress varies as PL increases (11, 12, 16). The implication of parenchymal deformability in real physiological circumstances is that neither the length of the smooth muscle nor the peribronchial stress is the independent variable; rather, PL is the independent variable. From the point of view of the muscle, therefore, deformability of the airway and the surrounding parenchyma may be thought of as being the source impedance, with changes of PL being the source.

In the literature (2, 5, 6, 8, 34), experiments on the effects of time-varying loads have been reported by using length control, which corresponds to applying an infinite source impedance to ASM; in this case, the servo-controlled lever arm applies whatever force might be required, no matter how large, to achieve the prescribed muscle length at a given time. Similarly, experiments have been reported that use force control, which corresponds to applying a zero source impedance (3). In such cases, the servo-controlled lever arm adjusts to whatever muscle length might be required to attain the prescribed force across the muscle at a given time.

Whereas force control is a closer approximation to physiological circumstances than length control, both loading strategies, as described below, are approximations that fail to take into account important aspects of the loading conditions that exist in realistic physiological conditions. In this study, we have used the known relationship between bronchial radius and peribronchial stress to create a time-varying virtual load impedance, simulating that presented to ASM by the airway wall and surrounding parenchyma.

The pressure difference across a cylindrical airway wall must be supported by radial and tangential (hoop) stresses within the wall. When those stresses vary appreciably across the wall thickness, the system is termed a "thick-walled" cylinder and the stresses are described by Lamé's equations; when those stresses are nearly constant across the wall thickness, the system is termed a "thin-walled" cylinder and Lamé's equations reduce to the law of Laplace (30). Traditionally, the literature on airway narrowing referred to above takes into account finite thicknesses of various wall compartments but does so within the context of the thin-walled cylinder approximation. Accordingly, forces within the airway wall (F_w) and force of the muscle (F_m) have units of force per unit of airway length and correspond to the integral of these tangential stresses across the finite thickness of the relevant airway compartment. We denote R as the instantaneous muscle radius (denoted by the mean of its inner and outer radii), in which case muscle length L is approximated by $2\pi R$. The forces developed by passive structures within the airway wall are $F_w(R)$, and the transmural pressure (P_{tm}) is the difference between the internal pressure and the peribronchial distending stress. F_w can be expressed as $\sigma_w h_w$, where σ_w is the average stress in passive structures and h_w is the thickness of those structures. Similarly, F_m can be expressed as $\sigma_m h_m$, where σ_{mus} is the average value of the active stress within the muscle compartment and h_m is the thickness of the muscle.

The law of Laplace describing the force that the muscle must generate, $F_m(R)$, in order for the muscle to attain a given radius R , takes the form

$$F_w(R) - F_m = P_{tm}R \quad (1)$$

We first consider $F_w(R)$. For the passive structures of the isolated airway, Lambert et al. (17) developed a semi-empirical expression relating R and P_{tm0} , where $F_w(R) = R P_{tm0}$,

$$\begin{aligned} R &= \sqrt{\alpha_0(1 - P_{tm0}/P_1)^{-n_1}} \quad P_{tm0} \leq 0 \\ R &= \sqrt{1 - (1 - \alpha_0)(1 - P_{tm0}/P_2)^{-n_2}} \quad P_{tm0} \geq 0 \\ P_1 &= \alpha_0 n_1 / \alpha'_0 \\ P_2 &= -n_2(1 - \alpha_0) / \alpha'_0 \end{aligned} \quad (2)$$

The values of the constants are determined to be $\alpha'_0 = 0.1125$, $P_1 = 0.1$, $n_1 = 0.045$, $P_2 = -20$, and $n_2 = 3$. It is also necessary to use the inverse of these functions

$$\begin{aligned} P_{tm0} &= P_1 \left[1 - \left(\frac{R^2}{\alpha_0} \right)^{-1/n_1} \right] \quad R \leq \sqrt{\alpha_0} \\ P_{tm0} &= P_2 \left[1 - \left(\frac{1 - R^2}{1 - \alpha_0} \right)^{-1/n_2} \right] \quad R \geq \sqrt{\alpha_0} \end{aligned} \quad (3)$$

Most authors now agree that there is probably a component of F_w that is attributable to buckling of the epithelial basement membrane (13, 14, 25, 32, 33, 35). The nature of the forces involved is currently unresolved because the mechanical properties of the basement membrane and submucosa and their mode of buckling collapse are not well established. There are conflicting opinions in the literature. One theoretical study suggests that, as the basement membrane thickens, the number of epithelial folds decreases and that, as the number of folds decreases, the load decreases and thereby promotes airway narrowing (35), whereas most studies suggest that thickening of the basement membrane tends to increase the load against which the muscle must shorten and thereby protects the airway from collapse (13, 14, 21, 25, 32, 33). Insofar as understanding of the role of this phenom-

enon is still emerging, and the load associated with the epithelium and submucosa was already a part of airways on which Lambert based his semi-empirical results (Eqs. 2 and 3), we call attention to the potential importance of muscle load associated with this wall compartment but do not attempt to model it explicitly in the present analysis.

We next consider P_{tm} , which can be computed from the work of Lambert and Wilson (16)

$$P_{tm}(R, P_L) = P_L - 2\mu(D_i - D)/D_i \quad (4)$$

where the shear modulus (μ) varies in direct proportion with the P_L as $\mu = 0.7 P_L$ (11, 12). The second term on the right side of Eq. 4 gives the component of the distending stress that is attributable to shear deformation of the lung parenchyma, where D_i denotes the diameter of the circular border between the airway adventitia and the surrounding lung parenchyma when the ASM is relaxed. D denotes the diameter of that same border when the smooth muscle has actively shortened. If it is assumed that all tissues are incompressible, then the adventitial cross section (A_a), is a constant. Taking the total airway crosssection ($\pi D_i^2/4$) as A_i , then the relationship between R and D was given by Lambert and colleagues (15) as

$$(D_i - D)/D_i = 1 - [A_a/A_i + (1 - A_a/A_i)(1 - (R_i - R)/R_i)]^{1/2}$$

when the muscle radius R departs from its undeformed reference radius R_i .

The system of equations above, taken together, define the force that the muscle must generate (F_m) to attain a given radius R . In the limit that the adventitial layer is small ($A_a = 0$), which is the case that we will treat here, D_i becomes $2R_i$, and the relationship simplifies to

$$F_m(R, P_L) = R \left[P_L + 2\mu \frac{(R_i - R)}{R_i} \right] - F_w(R) \quad (5)$$

Load characteristics defined by Eq. 5 are shown in Fig. 1 for a series of fixed P_L . Each sigmoidal line defines the auxotonic load against which ASM would have to shorten at a fixed P_L . During tidal breathing, however, P_L changes continuously in time, as does instantaneous load. The formulations of Lambert (Eqs. 2 and 3) and Lambert and Wilson (Eq. 4) ignore viscoelasticity and hysteresis of all passive structures.

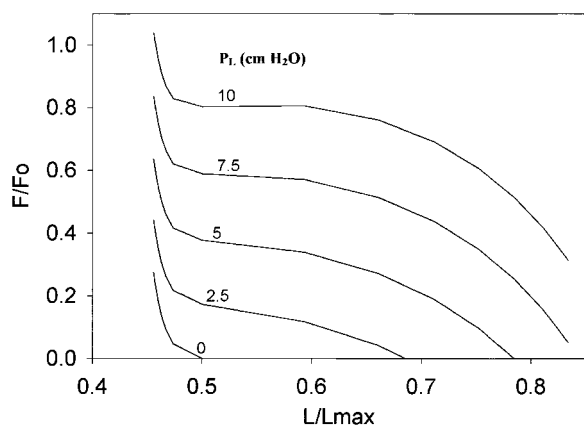


Fig. 1. The force-length load characteristic for transpulmonary pressures (P_L) of 0, 2.5, 5, 7.5, and 10 cmH_2O , dictated by Eq. 5. Each sigmoidal line defines the load against which airway smooth muscle would have to shorten at a fixed P_L . During tidal breathing, however, P_L changes continuously in time, as does the instantaneous load. F/F_0 , muscle force relative to optimal force; L/L_{\max} , muscle length relative to L_{\max} (length of relaxed muscle at a transpulmonary pressure of 30 cmH_2O).

Servo-controller. This load characteristic (Eq. 5) was integrated mathematically into our servo-controlled lever system to create, in the muscle bath, dynamic loading conditions that closely approximated those expected in vivo. A Labview program was written that receives force and length signals from a servo-controlled lever arm attached to a strip of ASM suspended in a bath. The length signal [normalized by the optimal length (L_0) described below] and the independently determined P_L were used to calculate the load to be applied to the muscle. We called L_{\max} the length of the relaxed muscle at a P_L of 30 cmH_2O and then set L_{\max} such that L_0 corresponded to 84% of L_{\max} . Because the lever arm is length controlled, a proportional-integrative-differential controller was used to convert the force differences to a length signal. This preparation is then made to breathe by varying the P_L in time.

Tissue preparation. Bovine tracheas were obtained from a local slaughterhouse, and a section of four to five rings in the caudal-to-central region of each was stored in cold phosphate-buffered saline for up to 24 h before use. The inner layer of connective tissue, adjoining cartilage, and outer connective tissue were carefully removed, and muscle strips measuring 2×10 mm were removed and the muscle dissected. Each end of the tissue strip was glued (cyanoacrylate) to small brass clips; insofar as this attachment method was entirely symmetrical from the point of view of the muscle, no bending or shear of the muscle was expected and, subsequently, no motions out of line with the applied forces were observed. The strip was then suspended in a glass tissue bath described previously (2) by using a fine steel rod (0.10-mm diameter). The top of the rod was attached to a servo-controlled lever arm via a miniature force transducer (Sensotec model MLB minigram beam load cell). The lower clip was latched onto a glass hook fused to the bottom of the bath. The bath was then perfused with a Krebs-Henseleit solution (in mM: 118 NaCl, 4.59 KCl, 1.0 KH_2PO_4 , 0.050 MgSO_4 , 0.18 CaCl_2 , 11.1 glucose, 23.8 NaHCO_3 ; pH 7.4), aerated with 95% O_2 -5% CO_2 , and maintained at 37°C by a surrounding water jacket.

In previous studies using this same apparatus in a force-control mode of operation, we calibrated the system with linear steel springs and were able to show that the effects of internal hysteresis in the apparatus and the effects of wires attached to the miniature force transducer were negligible (2, 3, 24).

Protocol. Quiet tidal breathing at rest would correspond to fluctuations of P_L from a minimum of ~ 3 cmH_2O at end expiration to a peak of ~ 6 cmH_2O at end inspiration; i.e., a peak-to-peak swing of 3 cmH_2O , corresponding to an amplitude of 1.5 cmH_2O with a mean of about 4 cmH_2O . In the studies reported here, we studied two values of the mean P_L : 5 and 2.5 cmH_2O .

After equilibration for 1 h, the strip was brought to L_0 in the standard manner using electric field stimulations adjusted for optimal response, beginning in the neighborhood of 20 V at 40 Hz for a 1.5-ms pulse duration for 30 s. Maximal tension was determined by activating the muscle with a dose of ACh (10^{-4} M) and allowing it to contract for 15 min. The bovine tracheal smooth muscle strip was then set in the muscle bath and loaded at a fixed (virtual) P_L of either 5 or 2.5 cmH_2O . The muscle was again activated with a high constant concentration of ACh (10^{-4} M) and allowed to shorten 120 min to its static equilibrium length (L_{SE}). After equilibration of the strip to static conditions, sinusoidal P_L fluctuations with amplitude δP_L (i.e., peak-to-peak excursion of $2\delta P_L$) and frequency were imposed on the muscle. After 60-min intervals to allow the muscle to become dynamically equilibrated at a new length, δP_L was increased from 10 to 25, 50, and 100% of the initial fixed P_L . After the largest

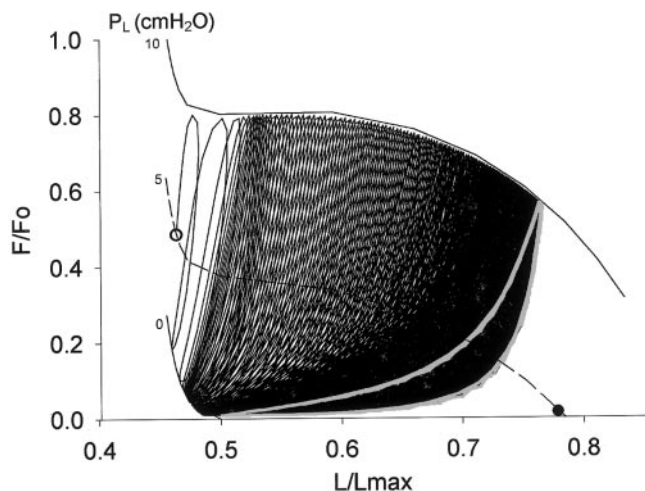


Fig. 2. For the relaxed muscle, the initial force and length are depicted by the \bullet at the lower right. When ACh was added, the muscle contracted auxotonically along the load characteristic corresponding to $P_L = 5$ cmH₂O until the muscle stopped shortening at the statically equilibrated state of the maximally constricted muscle (\circ at the left). Fluctuations of P_L (amplitude = 5 cmH₂O, mean = 5 cmH₂O) gave rise to force-length loops that spiraled down and to the right, slowly driving the muscle to progressively greater lengths and smaller forces. Eventually, a steady-state loop was observed (shown in gray). The dynamically equilibrated contractile state (grey loop) departed dramatically from the statically equilibrated contractile state (\circ).

fluctuation amplitude (100% of P_L) was completed, the fluctuation amplitude was returned to 25% of P_L and the muscle was allowed to reshorten.

RESULTS

Figure 2 depicts a representative tracing of F_m vs. muscle length. For the relaxed muscle, the initial force

and length are depicted by the closed circle at the lower right. When ACh was added to the bath and P_L was held constant at 5 cmH₂O, F_m increased and muscle length decreased; the muscle contracted auxotonically along the load characteristic corresponding to $P_L = 5$ cmH₂O until the muscle stopped shortening at the point indicated by the open circle at the left; this point represents the statically equilibrated state of the maximally constricted muscle. Accordingly, this is an important point of reference because it corresponds to the static equilibrium conditions that are assumed by classical theories of airway lumen narrowing (15, 19, 22).

After the activated muscle had become statically equilibrated, we imposed sinusoidal fluctuations of P_L , simulating the action of tidal breathing (amplitude of 5 cmH₂O, frequency of 0.2 Hz). These imposed fluctuations gave rise to force-length loops that spiraled down and to the right, slowly driving the muscle to progressively greater lengths and smaller forces; the time course is described in detail below. Eventually, a steady-state loop was observed (shown in gray in Fig. 2) that corresponded to the dynamically equilibrated state of the muscle for these particular loading conditions. The dynamically equilibrated contractile state departed dramatically from the statically equilibrated state.

A representative series of dynamically equilibrated force-length loops is shown in Fig. 3A. Also shown are corresponding traces of F_m vs. time (Fig. 3B) and muscle length vs. time (Fig. 3C). Although the mean P_L was held fixed at 5 cmH₂O, as the fluctuation about that mean was increased, the muscle came to progressively greater lengths and smaller mean forces; the steady-state loops were shifted down and to the right and were

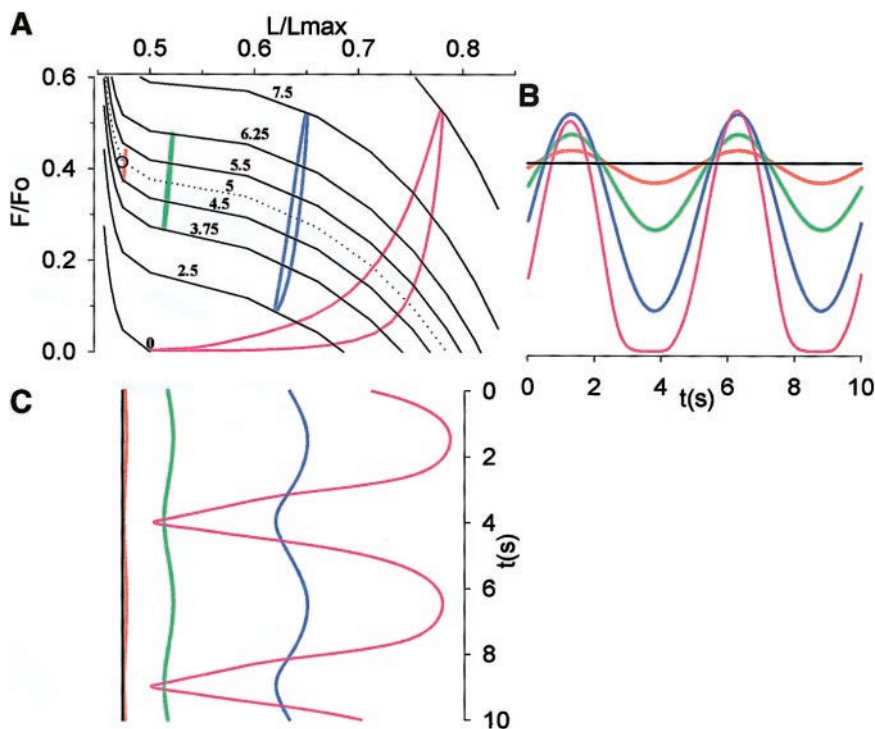


Fig. 3. A: the statically equilibrated state of the muscle (\circ , black line) and the steady-state loops for ASM dynamically equilibrated to pressure fluctuations of 0.5 (red line), 1.25 (green line), 2.5 (blue line), and 5 cmH₂O (pink line). B: corresponding traces of force vs. time (t). C: corresponding traces of length vs. time. Increasing fluctuations of P_L drove the muscle to greater lengths and lower forces.

less elliptical and more banana shaped. With increasing fluctuation amplitude, the minimum muscle force during the cycle became progressively smaller, whereas the peak force became progressively larger (Fig. 3A). This latter finding stands in contrast with the nearly fixed peak force that has been reported by using oscillations with simple length control (2, 5).

When sinusoidal fluctuations of P_L were <1 cmH₂O peak-to-peak, the corresponding length and force signals approximated sinusoids and fluctuated about their respective statically equilibrated values. However, as the sinusoidal fluctuations of P_L were increased beyond 1 cmH₂O peak-to-peak, the corresponding length and force signals became dramatically distorted away from sinusoids and became systematically biased toward greater average length and smaller average force (Fig. 3, B and C).

Trajectories of the force, length, stiffness, hysteresivity, and tidal strain (averaged over each tidal loop) are shown in Fig. 4 for a representative muscle strip. With the onset of the contractile stimulus, the force increased and the muscle length decreased. Although the initial shortening was quite rapid (Fig. 4, A), more than an hour was required for the muscle to reach its L_{SE} (Fig. 4, B); this time span is much longer than that required for muscle held in isometric conditions to reach a force plateau. Although muscle length equilibrated, F_m never established a clear plateau. As fluctuations in P_L were increased in a stepwise manner, F_m and muscle stiffness fell and muscle length and hysteresivity increased. The pooled steady-state data for a mean P_L of 5 cmH₂O are shown in Fig. 5.

The data described above, taken together, indicate that when the amplitude of the P_L fluctuation was increased from 0 to 0.5 cmH₂O, the instantaneous muscle state simply orbited the static equilibrium state. The mean muscle length and F_m over the cycle remained close to their static equilibrium values. But when pressure-fluctuation amplitude was increased to 1.25 cmH₂O or more, the force fell and the muscle lengthened and became progressively less stiff and more hysteretic (Figs. 3 and 4). Although the muscle was at all times supporting the same mean P_L (5 cmH₂O), the length to which the muscle equilibrated systematically exceeded the L_{SE} . Fluctuations of the P_L systematically biased ASM length.

If the amplitude of the tidal fluctuations of P_L was subsequently reduced from 5 back to 1.25 cmH₂O (Fig. 4, C), the muscle reshortened to a new length that was substantially greater than the prior length in identical loading conditions (triangles in Figs. 5 and 6). Therefore, the fluctuation amplitude necessary to maintain the muscle at that new length was smaller than that required to initially break through and attain that length. Conversely, if the fluctuations were kept at 1.25 cmH₂O or less throughout the contractile event, the muscle remained close to the L_{SE} , as if it were stuck at that length. The dynamic equilibrium length was determined by the tidal loading dynamics and, importantly, by the history of the tidal loading dynamics.

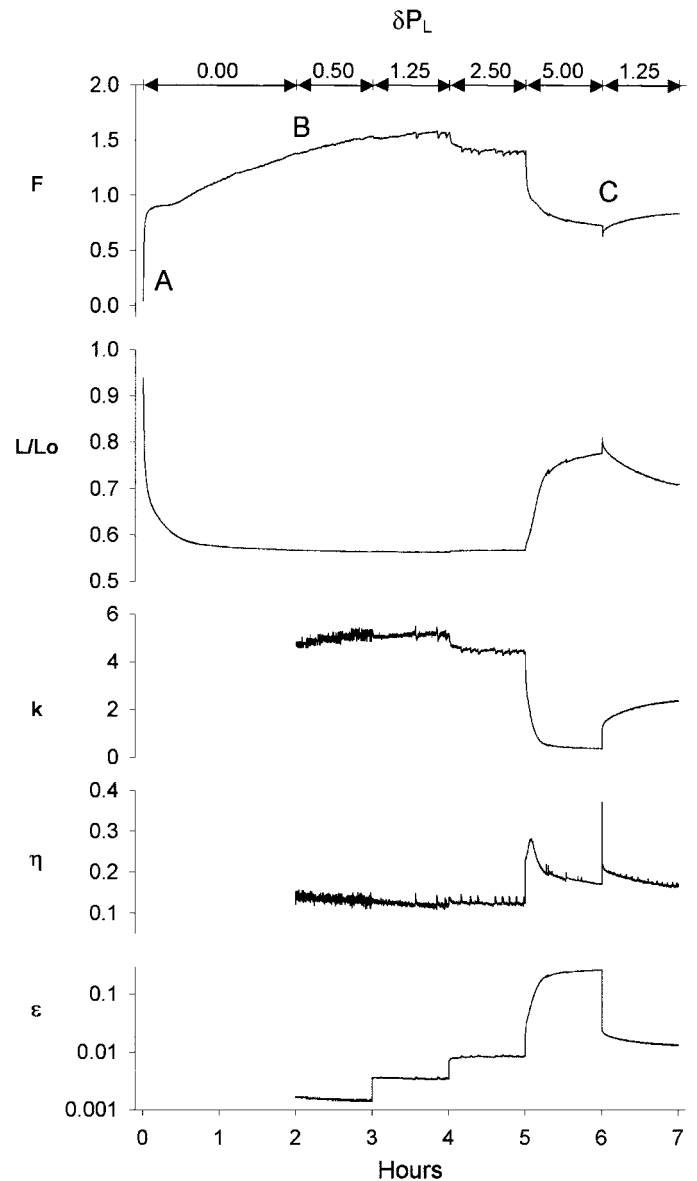


Fig. 4. Evolution of mechanical properties of a representative muscle during contraction against a steady mean P_L of 5 cmH₂O, on which is superimposed pressure fluctuations (0.2 Hz) of graded amplitude (δP_L ; cmH₂O). The mechanical properties shown are mean force (F ; arbitrary units), L/L_o , loop stiffness (k ; arbitrary units), hysteresivity (η ; dimensionless), and tidal strain (ϵ ; dimensionless). Pressure fluctuations are seen to drive the contractile state away from static equilibrium conditions. See text for definition of A–C (top).

When these experiments were repeated at a smaller mean P_L (2.5 cmH₂O), the dynamically equilibrated force and stiffness of the muscle were smaller and the hysteresivity was larger than at the higher mean P_L (Fig. 6). The smaller mean P_L had little effect on muscle length, however, probably due to the nature of the load characteristic, which was extremely steep at small muscle lengths.

After these tidal loading maneuvers, the isometric force generation capacity of the muscle was not compromised, retaining 85% or more of the initial capacity. Therefore, fluctuation-driven lengthening was not ac-

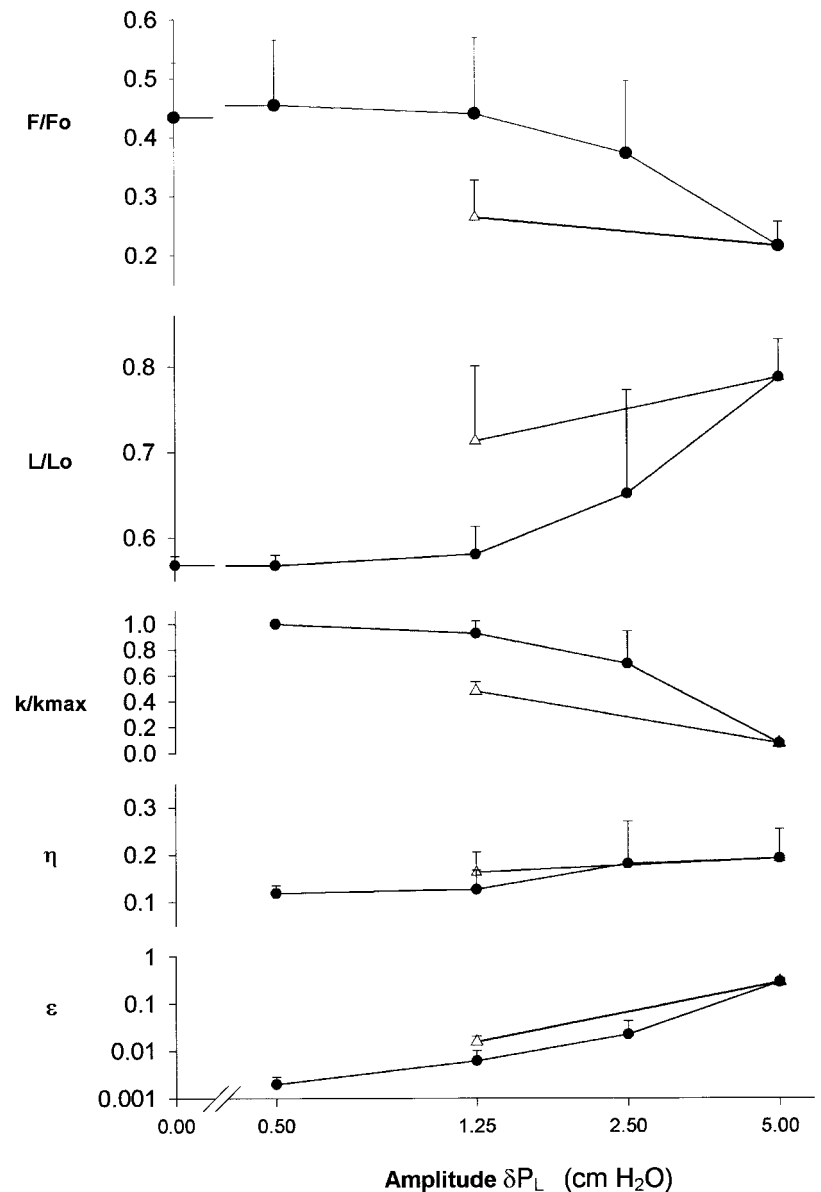


Fig. 5. Pooled observations for muscle strips with mean PL of 5 cmH₂O ($n = 5$; error bars denote SD between muscle strips drawn in only one direction for clarity) for dynamically equilibrated F/F_0 , L/L_0 , k relative to maximal k (k_{max} ; measured with smallest fluctuation amplitude δP_L), η , and ϵ . Δ , State after pressure fluctuations were reduced from 5 back to 1.25 cmH₂O.

counted for by muscle injury. Inouye (9) performed similar experiments using force control and found that once the muscle had become dynamically equilibrated (with a time constant close to 20 min), the subsequent duration of the forcing played little role compared with the amplitude.

DISCUSSION

We report here the development of a servo-controlled loading system that takes into account the nonlinear area-pressure relationship of the isolated airway, distortion of surrounding lung parenchyma, and the distending forces attributable to PL and its changes in time. This approach extends previous investigations of muscle contraction during time-invariant auxotonic loading (10, 18) to the case of a more physiological loading condition. Using this system, we employed a protocol that included as an unambiguous point of

reference the statically equilibrated muscle, which corresponds to the contractile state considered by classical theories of muscle shortening (15, 19, 22). The results indicate that the classical notion of statically equilibrated muscle behavior fails to approximate muscle behavior observed in a dynamic microenvironment that is thought to prevail in vivo. The principal findings of this report are that the maximally activated muscle becomes dynamically equilibrated at lengths that substantially exceed the L_{SE} and that the equilibration process is slow compared with the duration of one breathing cycle.

Although these studies relaxed important constraints of experimental loading systems that have been employed previously, there remain important limitations that warrant mention. First, we used sinusoidal fluctuations of PL, whereas quiet tidal breathing typically generates nonsinusoidal pressure traces

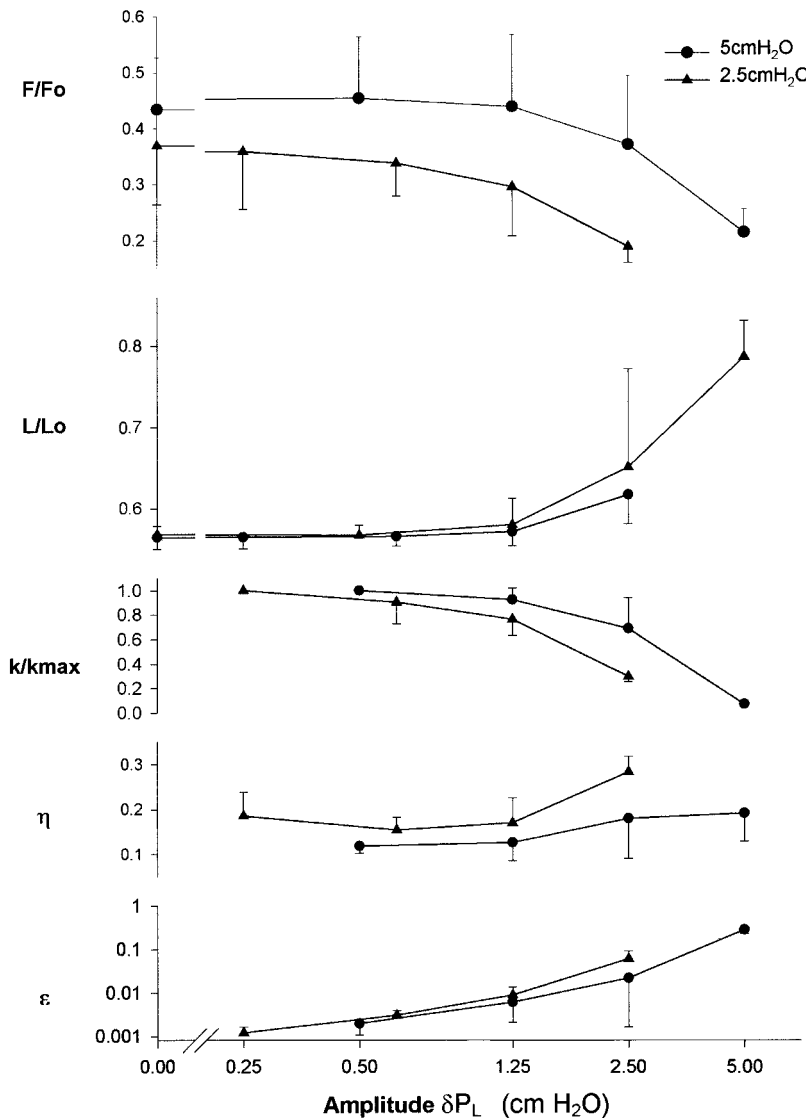


Fig. 6. Comparison of pooled observations for muscle strips with mean PL of 5 cmH₂O (●) vs. 2.5 cmH₂O (▲).

punctuated by occasional deep inspirations. Although any pattern of breathing could have been programmed into the servo-controller, we chose to limit attention to sinusoidal events for two reasons. Sinusoidal forcing makes it easier to appreciate distortions in force and length time histories that are induced by nonlinearities of the load characteristic and the muscle itself (Fig. 3). In addition, in prior studies that used force-control technology, we found that the muscle behavior is far less sensitive to changes of frequency than to changes in amplitude (9); as such, details of the waveform shape, which is governed by higher frequency harmonics, were not expected to have a substantial influence.

A second limitation of these studies is that we chose to impose pressure fluctuations about a mean PL that we held fixed, which stands in contrast with normal tidal breathing, which tends to have a fixed end-expiratory pressure (corresponding to functional residual capacity) with pressure excursions occurring above that floor. Although the normal pattern is clearly of interest, it leads to an interpretative ambiguity about

muscle behavior and mechanism that we sought to avoid. With the normal pattern of breathing, the mean PL (i.e., averaged over the breathing cycle) must increase in tandem with any increase of the amplitude of the fluctuation. As such, it would be less easy to discern what part of the muscle lengthening might be attributable to the dynamic part of the loading and what part might be attributable merely to the increased mean value of the load. Although they are somewhat less physiological than they might have been in that regard, these studies used a protocol in which the confounding effect of changes of the mean load was eliminated.

A third limitation concerns the order in which the interventions were applied. In these studies, we added a contractile agonist to the bath, allowed the muscle to shorten while the PL was held fixed and the muscle became statically equilibrated, and only then did we impose fluctuations of the PL. We chose this protocol because it defined an unambiguous point of departure, namely, the statically equilibrated contractile state

that would have been predicted by classical theories of muscle shortening, even after auxotonic shortening. By defining the protocol in this way, we were able to establish clearly that classical ideas about the statically equilibrated contractile state fail to account for muscle behavior in a dynamic microenvironment that approximates conditions thought to prevail *in vivo*. Alternatively, we might have begun with fluctuations of PL and then added the contractile agonist. Had we done so, the resulting dynamically equilibrated lengths might have been quite different, with those differences being attributable perhaps to plastic changes in the cytoskeleton induced by the fluctuations before addition of the agonist; phenomena of this type have been reported by Seow and colleagues (28, 31). The issue of the order of the interventions and their relationship to mechanism is important but goes beyond the scope of the present report.

The results reported here extend those that we reported earlier corresponding to simpler dynamic loading conditions, namely, force control that was length independent (3). In the force-control method, muscle force is specified and length must adapt accordingly. The extent of the fluctuation-driven muscle lengthening was smaller in the data reported here than in the force control method because the loading force decreased as muscle length increased; it is clear that force control is a good approximation only for those parts of the load characteristic that approach the horizontal (Fig. 1). Nonetheless, the dynamically equilibrated muscle length substantially exceeded the statically equilibrated muscle length when the tidal variations in PL exceeded an amplitude of 1.25 cmH₂O. This suggests that, even in the case of quiet tidal breathing, the effects of tidal respiration are important in maintaining airway caliber; this conclusion is consistent with the findings in human subjects by King et al. (10a).

To explain how the tidal action of lung inflations modulates smooth muscle function, our laboratory has previously put forward the theory of perturbed myosin binding (2). The results in the present study are consistent with that theory. The theory holds that lung inflation strains ASM with each breath. These periodic mechanical strains are transmitted to the myosin head and cause it to detach from the actin filament much sooner than it otherwise would have during an isometric contraction. This premature detachment profoundly reduces the duty cycle of myosin, typically to <20% of its value in the isometric steady state, and depresses to a similar extent total numbers of bridges attached and active force (3, 20). Of the full isometric force-generating capacity of the muscle, therefore, only a modest fraction comes to bear on narrowing the airway, even when the muscle is activated maximally. At the macroscopic level, the fully activated muscle is much less stiff and much more viscous than in an isometric contraction and, in effect, becomes a viscous liquid. At the molecular level, this liquid-like state corresponds to perturbed equilibria of myosin binding,

in which there are few cross links attached at any moment, but they are cycling very rapidly, almost as if the muscle had melted. Muscle length in that case would be dynamically equilibrated.

In pathological circumstances, however, the load fluctuations impinging on myosin can become compromised. For example, the chronically inflamed airway and the peribronchial adventitia remodel in way that is thought to uncouple the muscle from these load fluctuations (15); such an uncoupling would permit myosin to approach an unperturbed binding equilibrium, in which case the muscle would shorten, stiffen, and virtually freeze in the latch state (1, 3). In doing so, the myosin duty cycle would tend toward 100% of its value in isometric contraction. At the macroscopic level, the fully activated muscle is much more stiff and less viscous than in the melted state and becomes, in effect, a solid-like substance that is characterized at the molecular level by a static equilibrium of myosin binding in which there are many cross links attached at any moment, but they are cycling very slowly, almost as if the muscle had frozen. Muscle length in that case would be statically equilibrated.

In this study, we found that the dynamic equilibration process, which results from a sudden change in the amplitude of the fluctuations of PL, had a time constant in the range of tens of minutes, which is slow compared with the duration of one breathing cycle (Fig. 4). In contrast, we have previously reported that when length control is used to impose fluctuations of muscle length, the muscle becomes dynamically equilibrated very quickly, within one to three breaths (2). These seemingly disparate time scales required for the muscle to become dynamically equilibrated are reconciled by differences in the source impedance driving the muscle. In the case of length control, the servo-controller exerts whatever force is required to attain the assigned length at any instant and, in doing so, disrupts many attached bridges with the very first stretch. The myosin bond length distributions then adjust over time scales governed by bridge-attachment and -detachment rates, the slowest of which are on the order of seconds (20). By contrast, activated muscle that has become statically equilibrated is relatively stiff compared with the source impedance driving changes in muscle load *in vivo* and as modeled here. The muscle approximates a frozen state (3). Because it is so stiff, the muscle stretches relatively little when tidal changes of PL are initiated, and very few bridges are disrupted with the first breath. But the more it stretches, the easier it becomes to stretch. After many such breaths, the muscle gradually works loose, so to speak, and the binding of myosin to actin becomes strongly perturbed.

Although perturbed equilibria of myosin binding seem to be able to explain fluctuation-driven muscle lengthening and its time course, perturbed equilibria cannot explain the failure of the muscle to reshorten completely when the load fluctuations are removed,

and therefore this plasticity of the response must be attributable to other mechanisms (7, 23, 26, 29).

We thank the reviewers for helpful suggestions.

This work was supported by National Heart, Lung, and Blood Institute Grants HL-33009 and HL-59682.

REFERENCES

1. **Fredberg JJ.** Frozen objects: small airways, big breaths, and asthma. *J Allergy Clin Immunol* 106: 615–624, 2000.
2. **Fredberg JJ, Inouye D, Miller B, Nathan M, Jafari S, Raboudi SH, Butler JP, and Shore SA.** Airway smooth muscle, tidal stretches, and dynamically determined contractile states. *Am J Respir Crit Care Med* 156: 1752–1759, 1997.
3. **Fredberg JJ, Inouye DS, Mijailovich SM, and Butler JP.** Perturbed equilibrium of myosin binding in airway smooth muscle and its implications in bronchospasm. *Am J Respir Crit Care Med* 159: 1–9, 1999.
4. **Fredberg JJ, Jones KA, Nathan M, Raboudi S, Prakash YS, Shore SA, Butler JP, and Sieck GC.** Friction in airway smooth muscle: mechanism, latch, and implications in asthma. *J Appl Physiol* 81: 2703–2712, 1996.
5. **Gunst SJ.** Contractile force of airway smooth muscle during cyclic length changes. *J Appl Physiol Respir Environ Exercise Physiol* 55: 759–769, 1983.
6. **Gunst SJ.** Effect of length history on contractile behavior of canine tracheal smooth muscle. *Am J Physiol Cell Physiol* 250: C146–C154, 1986.
7. **Gunst SJ, Meiss RA, Wu MF, and Rowe M.** Mechanisms for the mechanical plasticity of tracheal smooth muscle. *Am J Physiol Cell Physiol* 268: C1267–C1276, 1995.
8. **Gunst SJ, Stropp JQ, and Service J.** Mechanical modulation of pressure-volume characteristics of contracted canine airways in vitro. *J Appl Physiol* 68: 2223–2229, 1990.
9. **Inouye D.** *Perturbed Equilibria of Myosin Binding in Airway Smooth Muscle and Its Implications in Airway Hyperresponsiveness and Asthma* (PhD Thesis). Cambridge, MA: Massachusetts Institute of Technology, Health Sciences, and Technology, 1999, p. 156.
10. **Ishida K, Pare PD, Blogg T, and Schellenberg RR.** Effects of elastic loading on porcine trachealis muscle mechanics. *J Appl Physiol* 69: 1033–1039, 1990.
- 10a. **King GG, Moore BJ, Seow CY, and Paré PD.** Airway narrowing associated with inhibition of deep inspiration during methacholine inspiration. *Respir Crit Care Med* 164: 216–218, 2001.
11. **Lai-Fook SJ.** Elasticity analysis of lung deformation problems. *Ann Biomed Eng* 9: 451–462, 1981.
12. **Lai-Fook SJ, Hyatt RE, and Rodarte JR.** Effect of parenchymal shear modulus and lung volume on bronchial pressure-diameter behavior. *J Appl Physiol* 44: 859–868, 1978.
13. **Lambert RK.** Role of bronchial basement membrane in airway collapse. *J Appl Physiol* 71: 666–673, 1991.
14. **Lambert RK, Pare PD, and Okazawa M.** Stiffness of peripheral airway folding membrane in rabbits. *J Appl Physiol* 90: 2041–2047, 2001.
15. **Lambert RK, Wiggs BR, Kuwano K, Hogg JC, and Pare PD.** Functional significance of increased airway smooth muscle in asthma and COPD. *J Appl Physiol* 74: 2771–2781, 1993.
16. **Lambert RK and Wilson TA.** A model for the elastic properties of the lung and their effects on expiratory flow. *J Appl Physiol* 34: 34–48, 1973.
17. **Lambert RK, Wilson TA, Hyatt RE, and Rodarte JR.** A computational model for expiratory flow. *J Appl Physiol* 52: 44–56, 1982.
18. **Li W and Stephens NL.** Auxotonic loading and airway smooth muscle shortening. *Can J Physiol Pharmacol* 72: 1458–1463, 1994.
19. **Macklem PT.** A theoretical analysis of the effect of airway smooth muscle load on airway narrowing. *Am J Respir Crit Care Med* 153: 83–89, 1996.
20. **Mijailovich SM, Butler JP, and Fredberg JJ.** Perturbed equilibria of myosin binding in airway smooth muscle: bond-length distributions, mechanics, and ATP metabolism. *Biophys J* 79: 2667–2681, 2000.
21. **Milanese M, Crimi E, Scordamaglia A, Riccio A, Pelligrino R, Canonica GW, and Brusasco V.** On the functional consequences of bronchial basement membrane thickening. *J Appl Physiol* 91: 1035–1040, 2001.
22. **Moreno R, Hogg JC, and Paré PD.** Mechanics of airway narrowing. *Am Rev Respir Dis* 133: 1171–1180, 1986.
23. **Morgan DL.** New insights into the behavior of muscle during active lengthening. *Biophys J* 57: 209–221, 1990.
24. **Navajas D, Mijailovich S, Glass G, Stamenovic D, and Fredberg JJ.** Dynamic response of the isolated relaxed rat diaphragm strip. *J Appl Physiol* 73: 2681–2692, 1992.
25. **Okazawa M, Pare PD, and Lambert RK.** Compliance of peripheral airways deduced from morphometry. *J Appl Physiol* 89: 2373–2381, 2000.
26. **Pratusevich VR, Seow CY, and Ford LE.** Plasticity in canine airway smooth muscle. *J Gen Physiol* 105: 73–94, 1995.
27. **Sasaki H and Hoppin FG Jr.** Hysteresis of contracted airway smooth muscle. *J Appl Physiol Respir Environ Exercise Physiol* 47: 1251–1262, 1979.
28. **Seow CY, Pratusevich VR, and Ford LE.** Series-to-parallel transition in the filament lattice of airway smooth muscle. *J Appl Physiol* 89: 869–876, 2000.
29. **Shen X, Wu MF, Tepper RS, and Gunst SJ.** Mechanisms for the mechanical response of airway smooth muscle to length oscillations. *J Appl Physiol* 83: 731–738, 1997.
30. **Uguzal A and Fenster S.** *Advanced Strength and Applied Elasticity*. London: Prentice-Hall, 1995. p. 328–334.
31. **Wang L, Paré PD, and Seow CY.** Effect of chronic passive length change on airway smooth muscle length-tension relationship. *J Appl Physiol* 90: 734–740, 2001.
32. **Wang L, Pinder KL, Bert JL, Okazawa M, and Pare PD.** Mechanical properties of the tracheal mucosal membrane in the rabbit. II. Morphometric analysis. *J Appl Physiol* 88: 1022–1028, 2000.
33. **Wang L, Tepper R, Bert JL, Pinder KL, Pare PD, and Okazawa M.** Mechanical properties of the tracheal mucosal membrane in the rabbit. I. Steady-state stiffness as a function of age. *J Appl Physiol* 88: 1014–1021, 2000.
34. **Warner DO and Gunst SJ.** Limitation of maximal bronchoconstriction in living dogs. *Am Rev Respir Dis* 145: 553–560, 1992.
35. **Wiggs BR, Hrousis CA, Drazen JM, and Kamm RD.** On the mechanism of mucosal folding in normal and asthmatic airways. *J Appl Physiol* 83: 1814–1821, 1997.